On the behaviour of steel CBF for industrial buildings subjected to seismic sequences

Giovanni Rinaldin *, Marco Fasan, Ljuba Sancin, Claudio Amadio

Department of Engineering and Architecture, University of Trieste, Piazzale Europa 1, 34127 Trieste, Italy

ARTICLE INFO

Keywords:
Seismic sequences
Hysteretic behaviour
Ductility demand
Non-linear SDOF systems
Concentric braced steel frame

ABSTRACT

The usual seismic design of buildings, based on current codes of practice, does not account for the occurrence of seismic sequences. Structures are designed to resist one single earthquake and then it is supposed that, before the following event, there is enough time to retrofit the damaged construction. This paper investigates the effects of seismic swarms on single storey Concentric X-Braced steel Frames, a very common construction system for industrial buildings. The selected seismic sequences have been chosen so that the first event is considered as the mainshock, and following events have a similar or greater PGA (Peak Ground Motion). The sequences can represent a swarm or a sequence of earthquakes spaced over time, occurring before the structures are retrofitted. The investigation of the effects on steel frames has been conducted in a simplified way through the analysis of Single Degree Of Freedom (SDOF) systems with a behaviour calibrated on the response of Multi-Degree Of Freedom (MDOF) real Concentrically Braced Frames (CBFs). One of the main focuses of this work is on the additional ductility to be used in the seismic design to account for the effects of seismic sequences. For this purpose, the 95th percentile of the required ductility ratio has been calculated in the typical fundamental frequency range of single storey concentric braced steel frames, as to estimate the increase of ductility or strength to be adopted in design. As a result, a reduction of behaviour factor up to 37% has been found.

1. Introduction

The seismic design of structures aims at designing safe buildings that resist, with or without damage, to the earthquakes that could occur in the site of construction. The most widespread design codes, such as Eurocode 8 [1], suggest to use a seismic input calibrated on a single seismic event, in the form of accelerograms or, more frequently, as response spectra. This design assumption does not account for the fact that, especially in regions with high seismicity, structures are often subjected to a sequence of earthquakes and not just to single events. If the time span between two consecutive earthquakes is not long enough to retrofit the buildings, the seismic sequence could lead to cumulative and not easily repairable damages. The effects of seismic sequences on structures should thus be better analysed and considered in codes of practice.

Some previous studies investigated different aspects of this issue, such as the characteristics of seismic sequences that affect buildings the most [2] and the effects of repeated ground motions on the non-linear response of bilinear Single Degree of Freedom (SDOF) systems [3], by using sequences made of repeated ground motions. One of the first studies about the additional ductility requested by seismic sequences to SDOF systems, compared to the demand of a single event, used artificial sequences generated by rational or random combination of real single events [4]. Di Sarno in 2013 [5] employed a rich set of records obtained from the earthquake sequence of Tohoku (Japan) to study a short list of earthquake response parameters in inelastic constant ductility spectra and force reduction factor spectra. Ruiz-Garcìa in 2014 [6] pointed out that the mainshock is always the event with the highest magnitude, but an aftershock could have a higher PGA for the site of interest - the critical seismic sequence is therefore a “far field mainshock – near fault aftershock” one. Some more studies investigated the behaviour of multiple degree of freedom (MDOF) systems subjected to seismic sequences. The response of bending resistant steel frames under repeated earthquake ground motions was analysed by Fragiacomo et al. in 2004 [7], while Ruiz-Garcìa [8] evaluated the drift demands in existing steel frames. The ductility demand [9] and the non-linear behaviour [10] of RC structures subjected to multiple earthquakes were also investigated. It was demonstrated that seismic sequences affect fragility curves of RC

* Corresponds to: Post-Doctoral Research Fellow.
E-mail addresses: grinaldin@units.it (G. Rinaldin), mfasan@units.it (M. Fasan), ljuba.sancin@phd.units.it (L. Sancin), amadio@units.it (C. Amadio).

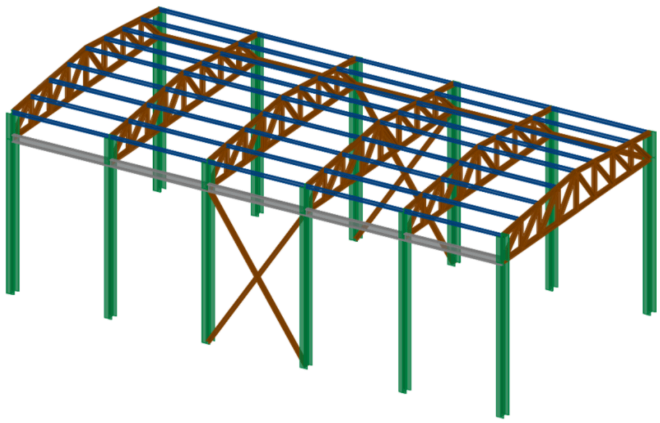

Fig. 1. Single storey concentric braced steel frame of a typical industrial building.

buildings [11]. Zhang et al. [12] studied a specific kind of structures by evaluating the damage of concrete gravity dams under mainshock-aftershock sequences.

Trutalli et al. [13] assessed the effects of non-dimensional slenderness in CBF framing systems, confirming the behaviour factor of 4 as in the current version of the Eurocode 8. The q factor seems to be only slightly affected by the slenderness used for designing the bracing if chosen in the range from 1.3 to 2.

Further studies have been developed on bracings systems, from their behaviour in progressive collapse [14] to the stiffening effects in RC buildings [15].

This paper is an extension of the research presented in [16], where some SDOF systems with different hysteretic behaviours are analysed under the action of multiple ground motions. In particular, in [16] the Elasto-Plastic (EP) model was used to represent the response of moment-resisting steel structures and it was investigated with and without hardening effect. The Pivot hysteretic law (PIV) was also used to represent the response of concrete and masonry buildings and it was investigated with a 5% softening plastic branch. It was found that the structures subjected to sequences should be designed for a higher ductility than the values currently provided by codes of practice for single seismic events. The ductility demand requested by the sequences was higher than the one of a single event and was depending on the resistance of the structure and on the kind of hysteretic behaviour.

In this paper, concentric X-braced steel frames are analysed, such as the frame in the longer side of the industrial building presented in Fig. 1. As known, typical single storey steel frames are composed of moment-resisting portal frames in the short direction and of braced frames in the long direction - the focus is on the last ones. A high elastic stiffness, a low energy dissipation capacity and relevant pinching effects, due to the instability of the compressed diagonals, characterize this construction system. Such features could lead to a very different response to after-shocks, compared to steel moment-resisting frames, which have already been deeply studied by many authors, as in Reinhorn [18]. Concentric braced steel frames (CBFs) are a widely used construction system and thus their behaviour should be carefully evaluated in order to allow an effective design in regions where it is typical to have seismic sequences. Both MDOF and SDOF systems that represent the behaviour of a real steel industrial structure were analysed, assuming always a single storey. In addition, recommendations of European [1] and Italian [19] codes of practice have been assumed. The major recommendation is about the limitation of non-dimensional slenderness, that must be limited to the range from 1.3 to 2 for X-braced concentric frames.

The increase in ductility requests or, conversely, the reductions for behaviour factors have been quantified for designing resilient braced frames.

In this study, we assumed to deal with well-designed single-storey braced frame, and the behaviour of gusset plates and connections is not accounted. The entire process is summarized on the workflow shown in Fig. 2.

2. Seismic sequences

The same sequences used in a previous work [16] have been adopted, so that the results obtained from this work can also be compared to the results of the SDOF systems calibrated on other kind of structures. Indeed, the SDOF analysed in this paper is representative of steel concentric braced frames and is modelled with a different hysteretic rule than the ones used in [16].

Therefore, ten seismic sequences have been used, all made of natural recorded earthquakes. The sequences have been chosen in such a way that the first event is considered as the mainshock and the following events have a similar or greater PGA (Peak Ground Motion) than the mainshock. Such sequences could lead to an increase in the ultimate displacement reached by the system, with a resulting increased demand for withstanding the seismic forces.

The sequences were built by assembling together all the single earthquakes of an event, with their real temporal order and by separating them with 60 s of zero acceleration, as shown in Fig. 3 for three

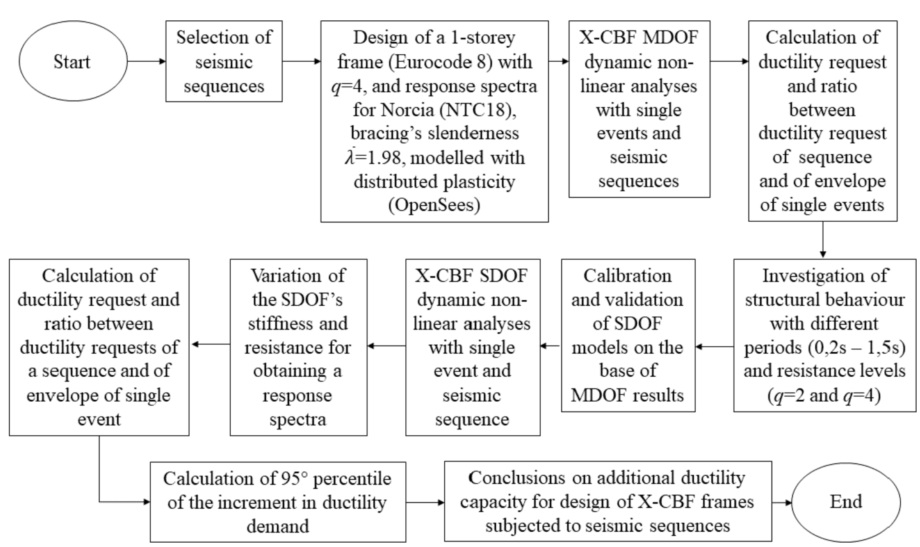

Fig. 2. Workflow of the analyses carried out.

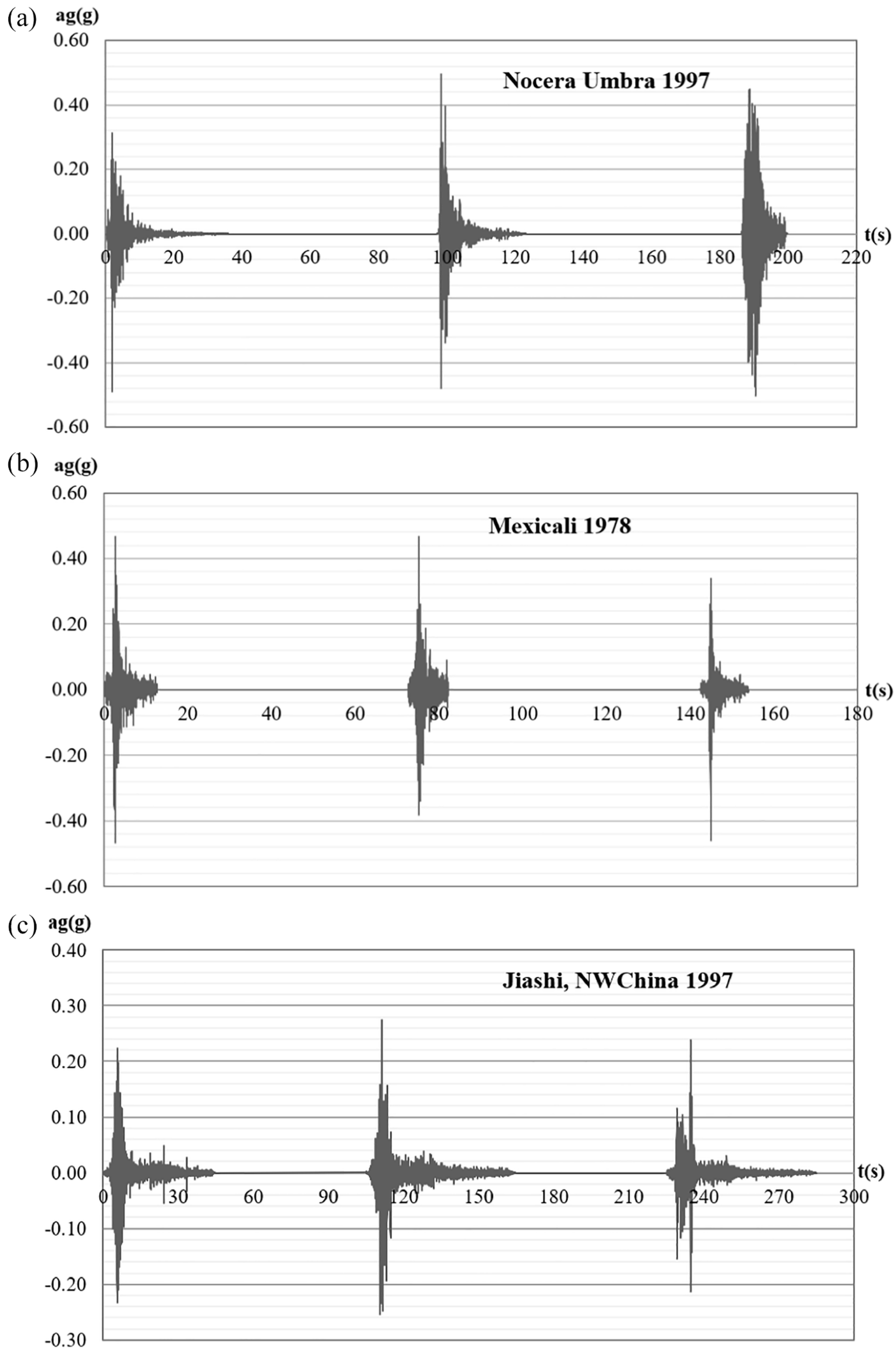

Fig. 3. Example of seismic sequences in terms of acceleration time-history: Mexicali (a), Nocera Umbra (b) and Noth-West China (c), all of them composed of three events separated by 60 s of zero acceleration.

sample cases: Mexicali, Nocera Umbra and North-West China. The 60 s of zero acceleration are chosen to assure that the system reaches a state of rest before the subsequent event occurs. The characteristics of the sequences are displayed in Table 1; each one is composed of 2, 3 or 4 single events. In the following, the single event of each sequence is named with its progressive temporal number. The time-histories are taken from on-line databases of natural records NIED [20], COSMOS [21] and ITACA [22].

Such seismic sequences can be categorized in three different groups (see column "Group" in Table 1):

A – The elastic spectrum of the sequence coincides with the spectrum of a single event;

B – The elastic spectrum of a single event is overlapped to the sequence spectrum only for a limited period range;

C – There is no dominant record in the sequence spectrum and all the single events contribute to the envelope.

This categorization, already adopted in [16] and [17], is described in the cited references.

Table 1
Characteristics of the 10 seismic sequences considered.

Group	Sequence	Date	Station name	Mw	Direction [N-S = 0°]	PGA [m/s^2]	Epicentral distance [km]	Focal depth [km]	Duration [s]
A	Christchurch	03/09/2010 16:35	CBGS	7.1	0°	−1.5101	36	10	110
		21/02/2011 23:51	CBGS	6.1	0°	5.5627	9.6	5.9	110
B	Nocera Umbra	10/06/1997 23:24	NCR	5.4	0°	−4.8129	11.1	5.5	37
		26/09/1997 00:33	NCR	5.7	0°	4.8588	13.2	5.7	29
		26/09/1997 09:40	NCR	6	0°	−4.9217	10.9	5.7	14
B	Mexicali Valley	11/03/1978 05:40	VCTRA	3.7	135°	4.5915	16	5.6	13
		11/03/1978 23:57	VCTRA	4.8	135°	4.578	2	6	10
		12/03/1978 00:30	VCTRA	4.5	135°	−4.515	7	6	12
B	Mendocino Cape	25/04/1992 11:06	Petrolia CA	7	0°	−5.7813	15.9	9.6	60
		26/04/1992 00:41	Petrolia CA	6.6	0°	5.8723	35.1	20	40
C	Chi Chi, Taiwan	20/09/1999 17:47	TCU129	7.6	90°	−9.8393	2.2	6.8	160
		20/09/1999 18:03	TCU129	6.2	90°	−9.3302	12.8	8	104
C	Niigata	23/10/2004 17:56	NIG020	6.6	0°	−5.2143	23.2	15.8	299
		23/10/2004 18:34	NIG020	6.3	0°	−5.2662	27.8	22.2	299
		25/10/2004 06:05	NIG020	5.7	0°	−4.2706	35.7	16.7	299
		27/10/2004 10:40	NIG020	6	0°	−5.231	18.8	15.7	299
C	NWChina	05/04/1997 23:46	Jiashi	5.9	270°	−2.2931	26.6	23.1	45
		11/04/1997 05:34	Jiashi	6.1	270°	2.685	27.7	20	60
		15/04/1997 18:19	Jiashi	5.8	270°	2.3451	33.6	22.4	60
C	Tohoku	11/03/2011 14:46	MYG001	9	0	4.1266	101	29	300
		07/04/2011 23:32	MYG001	7.1	0	3.8982	81.2	42	184
C	Hokkaido	29/11/2004 03:32	HKD071	7	0	2.7214	52.8	43.8	159
		06/12/2004 23:15	HKD071	6.7	0	2.9398	51.8	35.8	121
C	Weber	19/02/1990 05:34	120A	6.2	102°	1.4426	38	24.2	51
		13/05/1990 04:23	120A	6.4	102°	1.6475	33	12	54

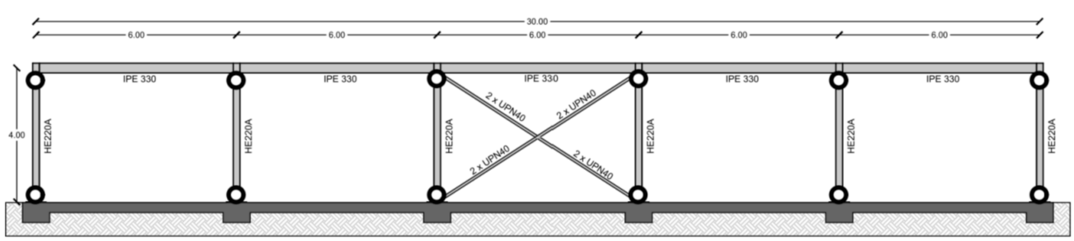

Fig. 4. Single storey X - braced steel frame, designed with $q = 4$. The pinned connections are indicated with empty circles.

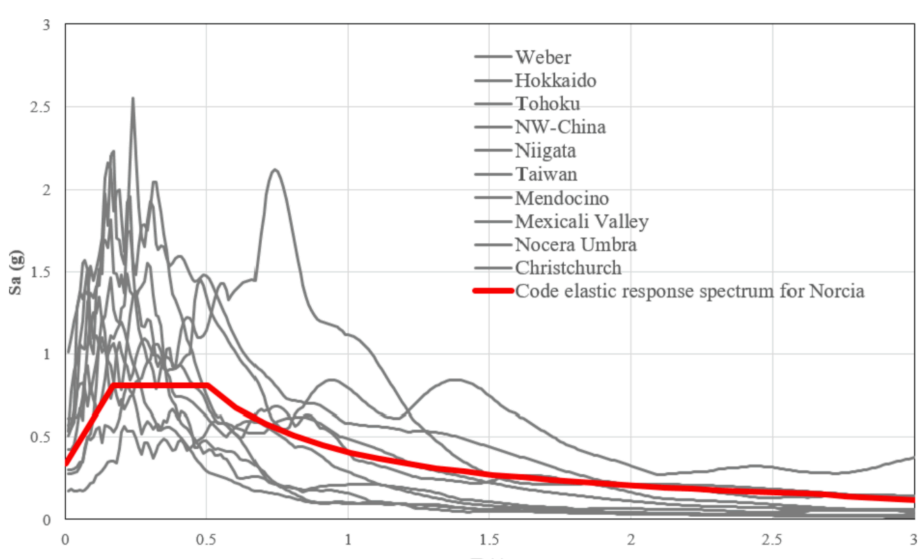

Fig. 5. Elastic response spectra of the 10 recorded seismic sequences and response spectrum at ULS as per code NTC 2018 for the site of Norcia (ground C).

3. Analysis of concentric X-braced steel frames with an MDOF system

X-braced frames are a very common form of construction, especially for industrial halls. They are affordable and have pinned connections that are simple to be realized. When subjected to seismic actions, the structure exhibits a good capacity, but the dissipation is not relevant, since it is just concentrated in the bracings. Moreover, the X-shape braces work just in tension and buckle in compression. Therefore, the cyclic behaviour of such constructions presents a typical pinching effect, causing a smaller energy dissipation.

A single storey frame with X-bracing, designed on the base of Eurocodes, has been investigated (see Fig. 4). The frame has been designed with linear static analysis in medium ductility class according to Eurocode 8 [1], by taking the upper limit of the reference value of behaviour factor for this type of structures $q = 4$. The frame has been designed by considering the response spectra given by the Italian design code (NTC2018) at Ultimate limit state (ULS) and Damage limit state (DLS) for the site of Norcia and for a reference life for the building of 50 years. The parameters chosen for calculating the response spectrum are: type of soil C and topography T3. The response spectrum used for the ULS is visible in Fig. 5, compared to the elastic response spectra of the 10 seismic sequences used in the analyses. The vertical static load applied to the beams, evaluated for the seismic combination, was set to 30 kN/m. The frame has been designed by taking into account all the code prescriptions, such as limitation on over-strength and capacity design rules.

The fundamental vibration period of this kind of structures is, in general, very short. In particular the analysed frame has a fundamental period of $T = 0.29$ s. The bracings of the X-braced frame are designed according to the prescription of Eurocode 8, (6.7.3) for which their non-dimensional slenderness $\overline{\lambda}$ should be limited to $1.3 < \overline{\lambda} \leq 2.0$(chosen $\overline{\lambda} = 1.98$). These limitations guarantee some dissipation and that buckling does not occur too early. The lower limit is needed not to overload the columns and frame joints with the compression transmitted by the diagonals.

The frame is modelled by using the OpenSees framework [232425]. All the connections (columns - foundation, beam - column, bracings) are considered as pinned, so that the bracings are the only elements that can resist horizontal load. This is an idealized model, as it does not consider the stiffness of real connections, that are usually not totally pinned and always have a small stiffness. In accordance with EC8 rules, connections possess an over-strength with respect to the bracing diagonals. Since the focus of the paper is on the additional required ductility, the secondary effects of real braced frames are thus not taken into account and the focus is made on the bracings. All the elements of the frame are modelled with distributed plasticity using the fibre section approach. The stress–strain relation for non-linear structural analysis assigned to the fibres is the Giuffrè-Menegotto-Pinto law with isotropic hardening, which is available in OpenSees library with the name of "Steel02". The following mechanical parameters were used for the fibre sections:

- Initial elastic modulus: 210 GPa;
- Yield strength: 277 MPa;
- Strain-hardening ratio: 0.015;
- Parameters for controlling the transition from elastic to plastic branches (in the same order as required by OpenSees): 20, 0.925, 0.15;
- Parameters for isotropic hardening (in the same order as required by OpenSees): 0, 1, 0.1, 1.

The steel frame is loaded vertically before subjecting it to seismic load. Dynamic non-linear analyses are then performed on the numerical model, by using the accelerograms of the single events and of the sequences. A mass-proportional damping factor of 5% has been adopted, consistently with the usual design procedures.

3.1. Numerical model for the bracings

As bracings are the fundamental part of the analysed structures, special attention is paid on their modelling. Like the whole structure, they are modelled with distributed plasticity and an elasto-plastic stress–strain relationship with 1% hardening is assigned to the fibres.

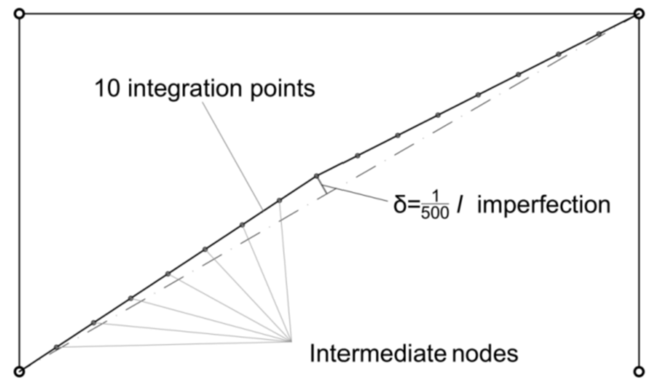

Fig. 6. Modelling characteristics for the representation of the bracings.

63 fibres are used for each section. The geometrical imperfections of the bracings and the second order effects are taken into account by the insertion of an initial imperfection $\delta = l/500$ in the middle of each bracing, as done in [26]. For a better simulation of the real behaviour, bracings are discretized in 16 elements with 10 integration points, as shown in Fig. 6.

The buckling of the compressed diagonal is crucial for the behaviour of the whole bracing system, and the slenderness of the diagonal is the main factor that affects buckling. The two diagonals composing the bracing are considered as not connected at mid-span.

The shape of the cyclic behaviour of an element with non-dimensional slenderness $\overline{\lambda} = 1.4$ can be found in literature, as reported in Fig. 7a. The validation of the numerical model is made on a single brace with slenderness $\overline{\lambda} = 2.0$. Comparing results in Fig. 7, it can be seen how the model reproduces faithfully the behaviour of a slender element, when subjected to dynamic loading.

3.2. Results for the MDOF braced system

The braced frame from Fig. 4 has been analysed by subjecting it to all the ten seismic sequences in Table 1. The ductility request is chosen as the main parameter for measuring cumulative damage. The ratio between the ductility request of the seismic sequence and the request of each single event is also calculated and, almost in all cases, there is an additional ductility demand by the sequence with respect to the upper envelope of the single events of 15%-20%, on average. Table 2 displays some examples of ductility demand for three seismic sequences (Mexicali, Nocera Umbra and NW China). δ_{min} and δ_{max} signify the minimum and the maximum horizontal displacements, respectively, while Δ_{max} is the overall maximum absolute displacement. Symbol μ is used for ductility measures. The values in the table are the results of the non-linear dynamic analyses performed on the MDOF system, where each element of the bracing system has been modelled as shown in Fig. 6. The additional ductility demand is due to the high stiffness of the structure and to the behaviour factor used in design. The reduction of resistance, due to the buckling of the compressed bracings, also affects the behaviour under seismic sequences.

Fig. 8 shows the cyclic behaviour of the single-storey X-braced frame under the action of the seismic sequence of Mexicali (the same graphs for the seismic sequences of Nocera Umbra and NW China are reported in Fig. 13 where they are compared to the hysteretic cycles of SDOF systems). The pinching effect due to the buckling of the diagonals is clearly visible in the graph. It can be also noticed that in some cases, as for instance in the Mexicali seismic sequence, the first event is the one with the major ductility demand, while, in other cases, the second or third earthquake have a higher demand.

Another important factor that affects the ductility demand is the residual displacement; the directionality of the seismic input is important to determine a higher or lower drift request in the events subsequent

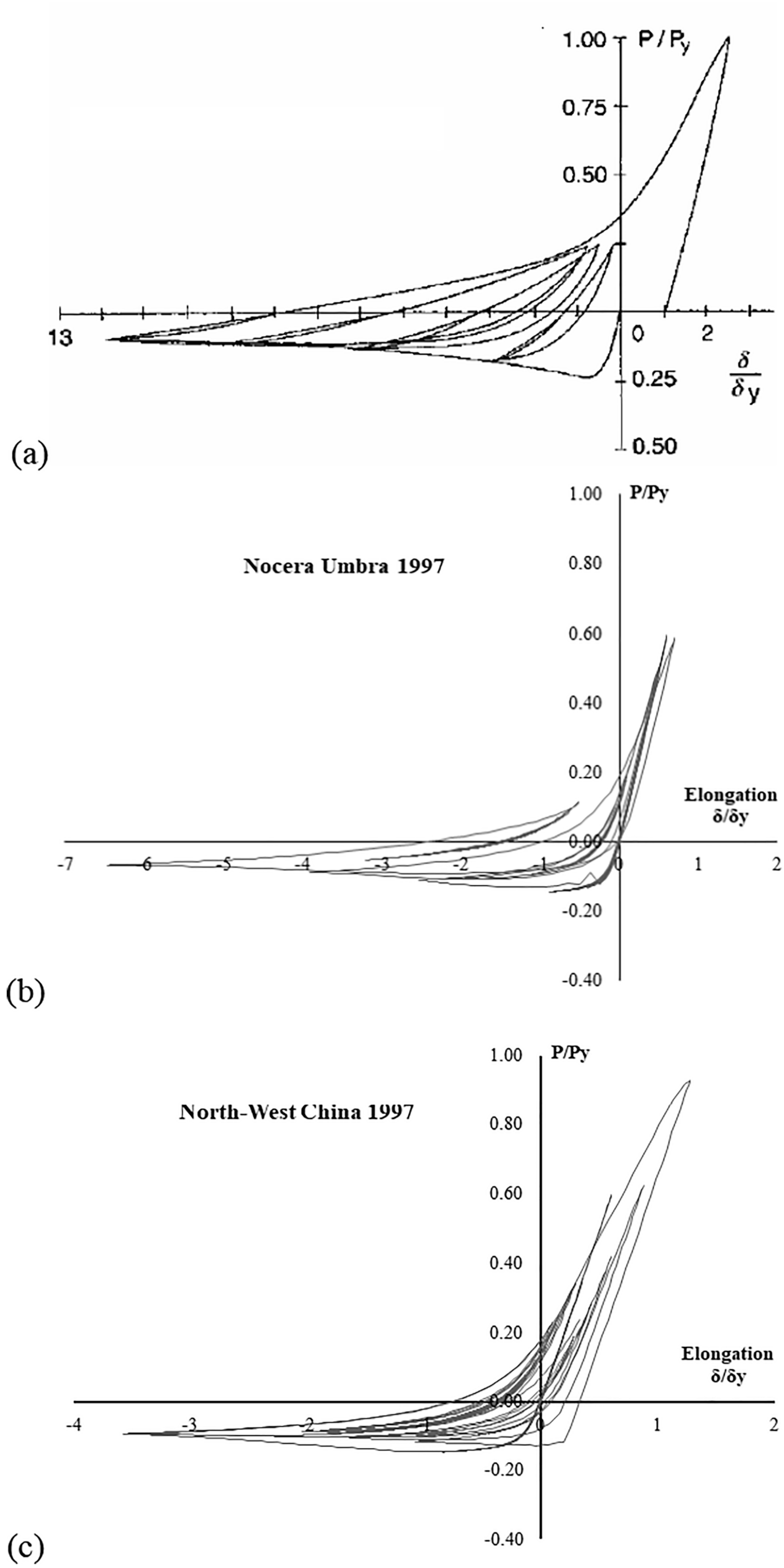

Fig. 7. Hysteretic behaviour of a slender brace (a) with $\overline{\lambda} = 1.4$, from [26], and cyclic behaviour of the single diagonal subjected to the seismic sequence of Nocera Umbra (a) and NW China (b).

Table 2
Examples of calculation of the additional ductility demand by the seismic sequences compared to the maximum single event, for the X-braced single storey frame.

MDOF (X - bracing)			
Mexicali	δ_{min} [cm]	δ_{max} [cm]	Δ_{max} [cm]
Event 1	−1.54	1.39	1.54
Event 2	−0.74	0.92	0.92
Event 3	−0.81	1.00	1.00
Seq123	−1.54	1.39	1.54
$\mu_{sequence}$ / $\mu_{max\ single\ event}$			1.00
$\mu_{sequence}$ / $\mu_{event\ 1}$			1.00
MDOF (X - bracing)			
Nocera Umbra	δ_{min} [cm]	δ_{max} [cm]	Δ_{max} [cm]
Event 1	−0.97	0.61	0.97
Event 2	−1.12	0.66	1.12
Event 3	−2.57	1.49	2.57
Seq123	−2.76	2.19	2.76
$\mu_{sequence}$ / $\mu_{max\ single\ event}$			1.07
$\mu_{sequence}$ / $\mu_{event\ 1}$			2.85
MDOF (X - bracing)			
NW China	δ_{min} [cm]	δ_{max} [cm]	Δ_{max} [cm]
Event 1	−2.00	2.03	2.03
Event 2	−2.57	1.22	2.57
Event 3	−1.59	1.52	1.59
Seq123	−4.66	2.34	4.66
$\mu_{sequence}$ / $\mu_{max\ single\ event}$			1.81
$\mu_{sequence}$ / $\mu_{event\ 1}$			2.29

to the first. As shown in Fig. 9, the residual displacement after each event remains in the positive or negative direction on the X-axis, and it is not predictable in advance, hence the structure is not re-centred before the subsequent earthquake starts. This can lead to a minor ductility demand if the maximum displacement is in the opposite direction, or a higher demand if the maximum displacement is in the same direction of the residual one. As an example, the case of the single floor frame, subjected to Nocera Umbra and NW China seismic sequences is presented in Fig. 9.

3.3. Comments on results for MDOF systems

The results obtained from the analysis of the MDOF system show that concentric braced steel frames are more sensitive to seismic sequences than moment-resisting frames [16] and they exhibit almost in all cases a higher ductility demand when subjected to repeated ground motion.

Table 3 reports the maximum and residual displacements for the selected sequences. As expected, the residual displacements are always lesser than the maximum ones reached during the analysis with the whole sequence.

The main weakness of the analysed MDOF is that it represents just structures with the same fundamental vibration period - in other words, every single structure corresponds to just one point on a response spectrum. In order to generalize the findings, it is necessary to check what happens in the whole range of periods that similar structures may have. Moreover, the different levels of resistance of the structure is a parameter that could strongly affect the final behaviour and should thus be investigated. The easiest way to investigate a whole range of periods and different levels of resistance is to perform analyses on SDOF systems that well represent the MDOF structures of interest [27]. In this paper it was chosen to analyse SDOFs with a hysteretic rule that accounts for pinching effect. The range of periods between *0.2 s* and *1.5 s* is investigated, for two different levels of resistance (strength reduction factors f = 0,5 and f = 0,25 are chosen as the inverse value of the ductility levels of 2 and 4) and the ductility demand is found.

4. SDOF representation of the MDOF system

In the previous paragraph it has been pointed out that the non-linear seismic response of concentric-braced steel frames has pinching effect as a fundamental characteristic. When trying to approximate the behaviour of such MDOF systems with a SDOF model, this fundamental characteristic should be taken into account.

For this purpose, the OpenSees framework [232425] is used to carry-out non-linear dynamic analyses on SDOF systems built as shown in Fig. 10. The model is composed of a rigid beam with unitary length *h* and mass m^* at the top, connected to the floor through a pinned joint and a rotational spring with stiffness K^*. The rotational spring is characterized by the moment-rotation (M – ϕ) law of the "Hysteretic Uniaxial Material" [28], which can be found in the software library and is depicted in Fig. 11. This hysteretic rule has the desired pinching effect and the parameters of the cycle are set for the best fit with the behaviour of the MDOF system. The parameters for the definition of pinching effect are:

- *pinchX*: pinching factor for strain (or deformation) during reloading;
- *pinchY*: pinching factor for stress (or force) during reloading.

As can be seen from Fig. 11, the parameters defining the backbone curve are:

- ϕ_{yp} , M_{yp}: rotation and moment at first point of the envelope in the positive direction;
- ϕ_{up} , M_{up}: rotation and moment at second point of the envelope in the positive direction;

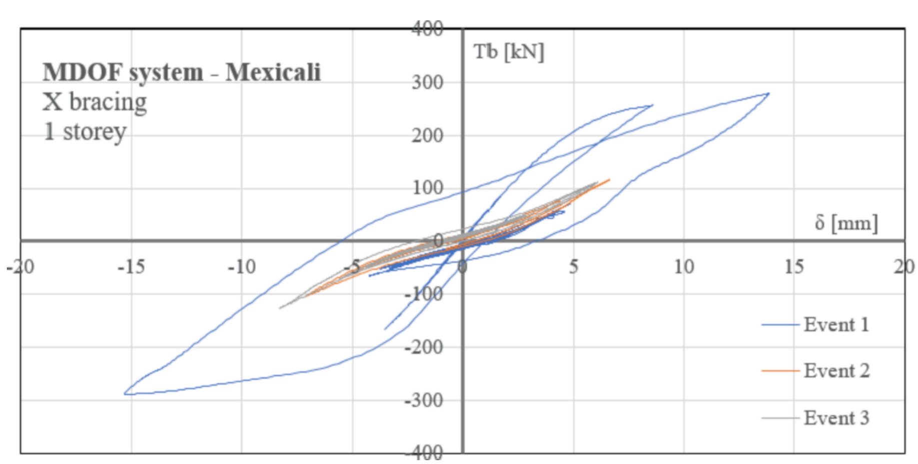

Fig. 8. Result of the non-linear dynamic analysis performed on the single storey X-braced structure, in terms of base shear – displacement.

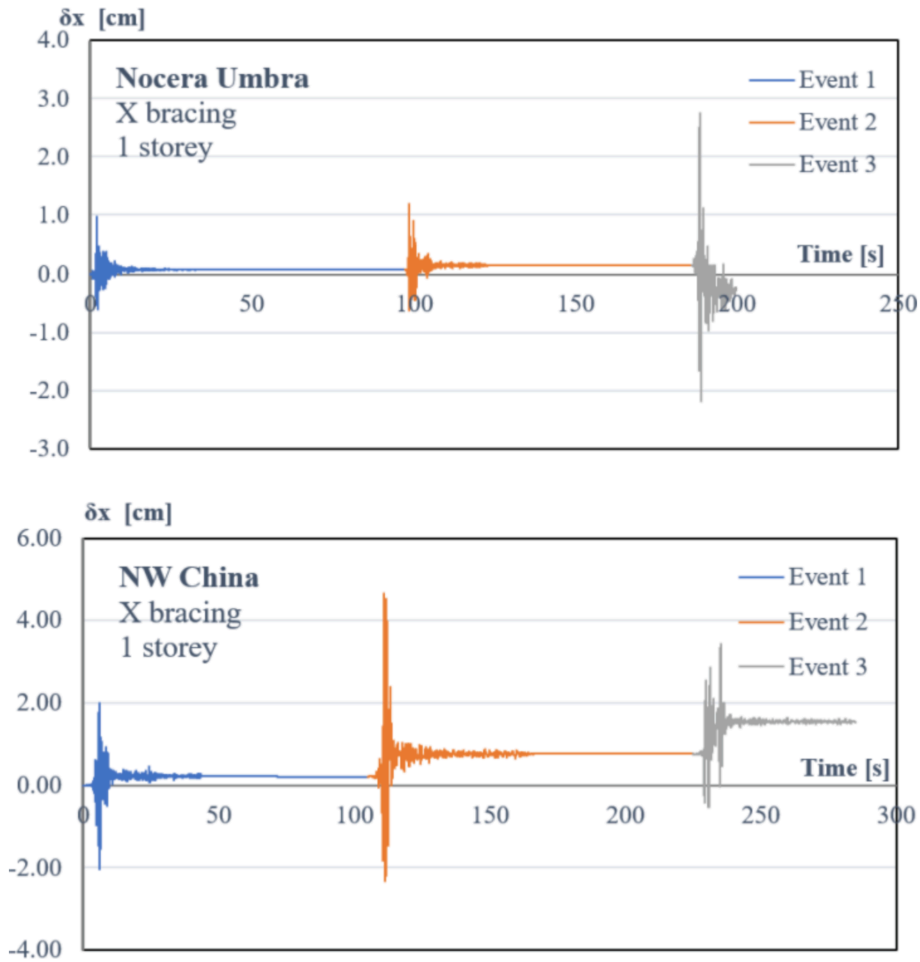

Fig. 9. Time-displacement graphs for the single storey X-braced steel frame, subjected to Nocera Umbra and NW China sequences.

Table 3
Absolute maximum and residual displacements of the MDOF systems for NW China, Nocera Umbra and Mexicali sequences.

Sequence name	Δ_{max} [cm]	Δ_{res} [cm]
NW China	4.66	1.54
Nocera Umbra	2.76	0.28
Mexicali	1.54	0.06

- ϕ_{yn} , M_{yn}: rotation and moment at first point of the envelope in the negative direction;
- ϕ_{un} , M_{un}: rotation and moment at second point of the envelope in the negative direction.

The parameters used to approximate the behaviour of the MDOF system, more specifically the X – braced structures, are the ones shown in Table 4. Other parameters of the described hysteretic material that are not in Table 4 (see [27]) were taken as 0.

A sample of the result obtained in terms of base shear force V versus the top displacement δ is shown in Fig. 12 for the seismic sequence of Mendocino Cape.

4.1. Validation of equivalent SDOF system

The approximation of the behaviour of MDOF systems with a SDOF model can be evaluated by comparing the cycling behaviour of both systems, subjected to the ten seismic sequences. Such comparison is reported in Fig. 13 for the single storey X-braced frame with vibration period $T = 0.29$ s. The maximum displacements and the ductility ratios are numerically compared in Table 5. As can be noticed, the displacements of the SDOF system are comparable with the ones from MDOFs, and the shape of the hysteretic rule reasonably represents the pinching effect and the plasticization of the compressed bracing.

5. Characterisation of the SDOF systems for response spectra

Since the chosen hysteretic rule is representative of the concentric X-braced steel frame, SDOF systems with this behaviour but with different vibration periods and resistances are analysed, as to obtain a response spectrum. It must be emphasized that design rules force the slenderness to be within a limited range of values. This implies that the hysteretic cycles cannot vary much and that the variations in the vibrational period are mainly due to the variation in the mass of the buildings. To investigate the cumulative damage, it is necessary to ensure the plasticization of the system; for this reason, the yielding resistance of each SDOF system, given in OpenSees by the parameter M_{yp} (see Fig. 11), is set based on the characteristics of the ground motion, through the reduction factor f to be applied to the maximum seismic force. The strength reduction factors f considered in this work are the same as in [16], so that the results can be easily compared. They are chosen equal to the inverse value of the ductility levels of *2* and *4*, thus $f = 0.5$ and $f = 0.25$. The parameter M_{yp} is therefore set as in Eq. (1):

$$\frac{M_{yp,i}}{h} = F_{yp,i} = f \cdot F_{e,i} = f \cdot S_{a,elastic}(T_i) \cdot m \tag{1}$$

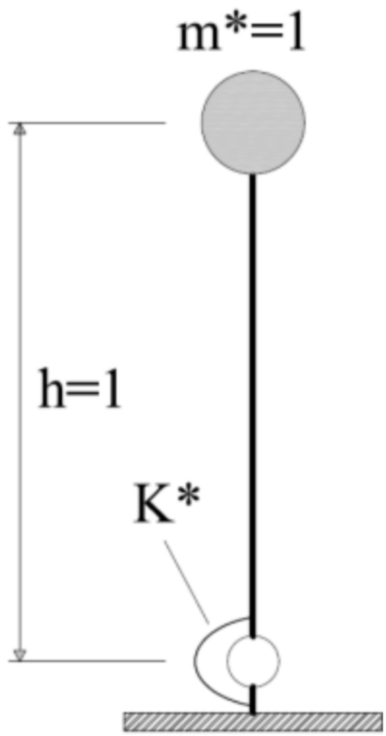

Fig. 10. Scheme of the SDOF system modelled through a rigid beam with unitary length h, mass m^* and a flexural spring with stiffness K^*.

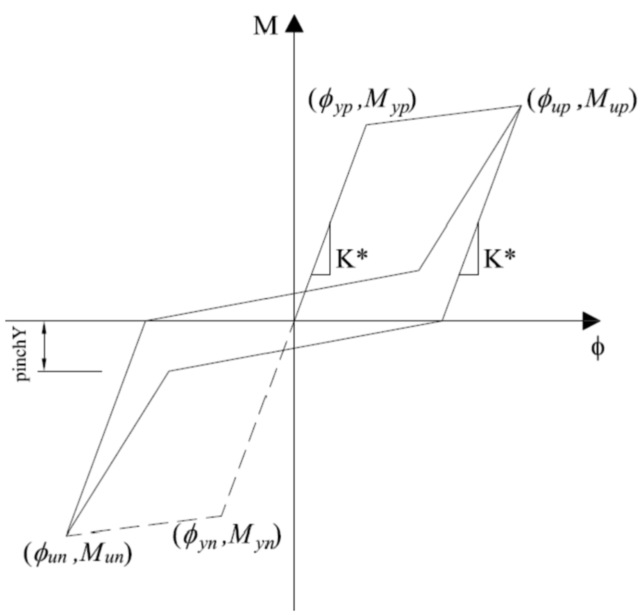

Fig. 11. Hysteretic cycle available in OpenSees, where K^* is the stiffness of the system.

Table 4
Parameters used for SDOF systems.

Resisting moments [kNm]		*Corresponding rotations [rad]*		*Pinching effect parameters*	
M_{yp}	300	ϕ_{yp}	0.005	*pinchX*	0.8
M_{up}	320	ϕ_{up}	0.10	*pinchY*	0.2
M_{yn}	−300	ϕ_{yn}	−0.005		
M_{un}	−320	ϕ_{un}	−0.10		

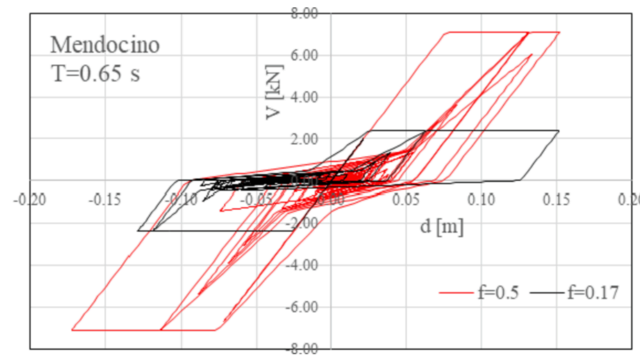

Fig. 12. Hysteretic rule for the material "Hysteretic UniaxialMaterial" available in OpenSees, with $pinchX = 0.8$ and $pinchY = 0.2$.

where $M_{yp,i}$ denotes the yielding strength of the SDOF system with vibration period T_i, h is the unitary height, $F_{e,i}$ is the elastic force required by the elastic spectrum, $S_{a,elastic}(T_i)$ is the elastic spectral acceleration for the *i-th* vibration period and m signifies the unitary mass.

It has to be pointed out that, in order to compare the results found for the single seismic event with the results from the seismic sequence, the $S_{a,elastic}(T_i)$ is always taken from the response spectrum of the sequence, and not from the response spectrum of the single event. The elastic response spectra are also calculated using OpenSees, giving as input the time history of the acceleration of the ground motion for each seismic sequence. All the analyses are carried-out considering a damping ratio of *0.05*. The range of investigated natural vibration period goes from *0.20 s* to *1.50 s*, with steps of *0.01 s*.

The stiffness of each SDOF system, K^*, is determined from the desired vibration period, T, through the equation:

$$K^* = m \cdot \omega^2 \tag{2}$$

where $\omega = 2\pi/T$ and m is the unitary mass.

The parameters for the SDOF analysis are reported in Table 6.

6. Results from SDOF systems

The aim of this study is to check if the results found on the MDOF steel braced frame system are general. It was found that this kind of structures require in some cases a significant additional ductility when subjected to seismic sequences, compared to a single event.

In order to make this result as general as possible, SDOF systems with the hysteretic rule described above are analysed and the ductility demand is calculated for each single event and for the whole sequences, and for each strength reduction factor f considered. With the purpose to evaluate the additional ductility demand of the seismic sequences, the ratio r_μ between the seismic sequence ductility demand $\mu_{r,seq}$ and the envelope of ductility $\mu_{r,env}$ requested by each single event is chosen:

$$r_\mu = \frac{\mu_{r,seq}}{\mu_{r,env}} \tag{3}$$

With the aim to find a guideline value for the design of structures subjected to seismic sequences, the 95th percentile of the increment in ductility demand is calculated for each strength reduction factor. This value could be considered as a characteristic value, as usual in codes of practice.

From the graphs in Fig. 14 and the values in Table 7, it can be noticed how lower vibration periods have a higher ductility ratio than longer periods, especially for more resistant structures ($f = 0.5$, that could be associated with a behaviour factor $q = 2$). Therefore, the vibration period range taken for the calculation of the 95th percentile highly affects the resulting value. For this reason, the percentile is calculated in several period ranges. It has to be pointed out that, since steel framed structures, which are represented by the analysed SDOF systems, have a

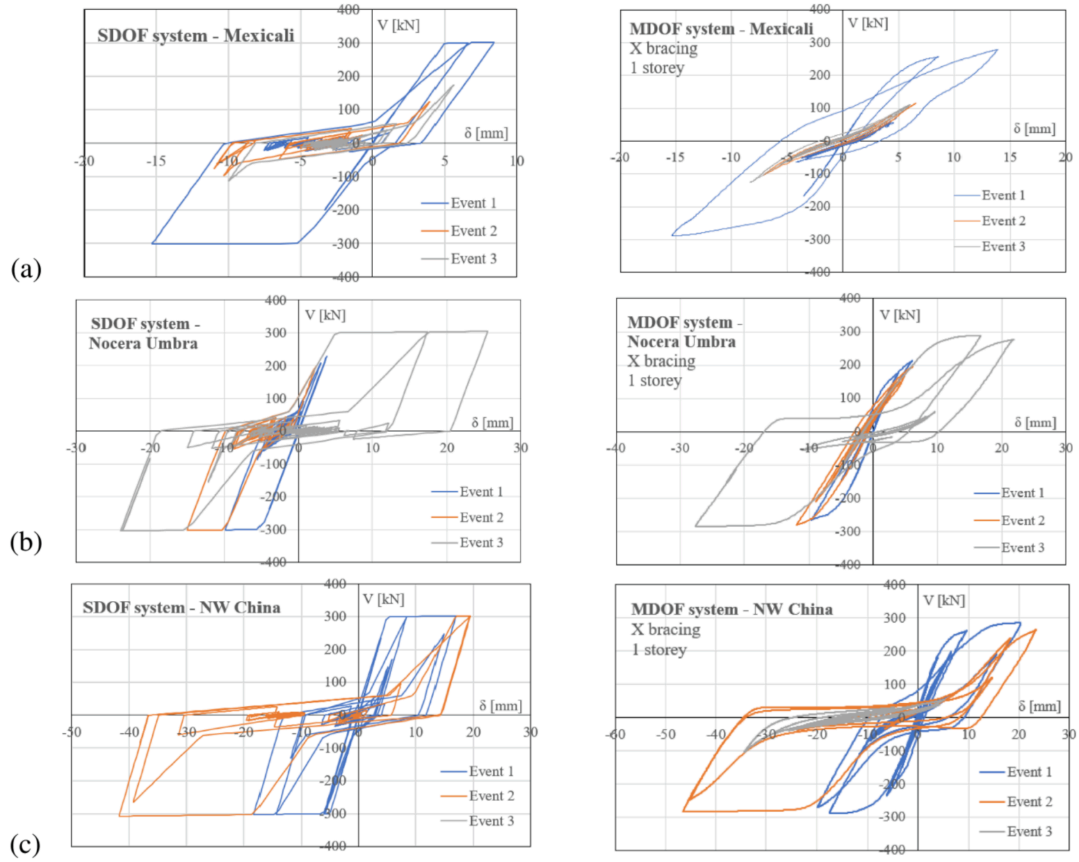

Fig. 13. Base shear – displacement graphs for the SDOF system (left) and the MDOF system (right) associated to the single storey X-braced frame, subjected to Mexicali (a), Nocera Umbra (b) and North West China (c) seismic sequence.

Table 5
Maximum displacements of the MDOF and SDOF systems and related ductility ratios.

MDOF (X - bracing)				SDOF			
NW China	δmin [cm]	δmax [cm]	Δmax [cm]	NW China	δmin [cm]	δmax [cm]	Δmax [cm]
Event 1	−2.00	2.03	2.03	Event 1	−1.83	1.69	1.83
Event 2	−2.57	1.22	2.57	Event 2	−2.61	0.59	2.61
Event 3	−1.59	1.52	1.59	Event 3	−1.36	1.14	1.36
Seq123	−4.66	2.34	4.66	Seq123	−4.18	1.95	4.18
$\mu_{sequence} / \mu_{max\ single\ event}$			1.81	$\mu_{sequence} / \mu_{max\ single\ event}$			1.60
$\mu_{sequence} / \mu_{event\ 1}$			2.29	$\mu_{sequence} / \mu_{event\ 1}$			2.29
MDOF (X - bracing)				SDOF			
Nocera Umbra	δmin [cm]	δmax [cm]	Δmax [cm]	Nocera Umbra	δmin [cm]	δmax [cm]	Δmax [cm]
Event 1	−0.97	0.61	0.97	Event 1	−0.99	0.38	0.99
Event 2	−1.12	0.66	1.12	Event 2	−1.09	0.53	1.09
Event 3	−2.57	1.49	2.57	Event 3	−2.38	1.38	2.38
Seq123	−2.76	2.19	2.76	Seq123	−2.40	2.55	2.55
$\mu_{sequence} / \mu_{max\ single\ event}$			1.07	$\mu_{sequence} / \mu_{max\ single\ event}$			1.07
$\mu_{sequence} / \mu_{event\ 1}$			2.85	$\mu_{sequence} / \mu_{event\ 1}$			2.59
MDOF (X - bracing)				SDOF			
Mexicali	δmin [cm]	δmax [cm]	Δmax [cm]	Mexicali	δmin [cm]	δmax [cm]	Δmax [cm]
Event 1	−1.54	1.39	1.54	Event 1	−1.53	0.84	1.53
Event 2	−0.74	0.92	0.92	Event 2	−0.69	0.85	0.85
Event 3	−0.81	1.00	1.00	Event 3	−0.68	1.05	1.05
Seq123	−1.54	1.39	1.54	Seq123	−1.53	0.84	1.53
$\mu_{sequence} / \mu_{max\ single\ event}$			1.00	$\mu_{sequence} / \mu_{max\ single\ event}$			1.00
$\mu_{sequence} / \mu_{event\ 1}$			1.00	$\mu_{sequence} / \mu_{event\ 1}$			1.00

Table 6
Parameters for the definition of the hysteretic rule of the SDOF systems in OpenSees.

Resisting moments [kNm]		*Corresponding rotations [rad]*		*Pinching effect parameters*	
M_{yp}	$F_{y,i}$	ϕ_{yp}	F_{yp}/K	pinchX	0.8
M_{up}	$F_{y,I} \cdot 1.1$	ϕ_{up}	$200 \cdot d_{yp}$	pinchY	0.2
M_{yn}	$-F_{y,i}$	ϕ_{yn}	$-d_{yp}$		
M_{un}	$-F_{y,I} \cdot 1.1$	ϕ_{un}	$-d_{up}$		

high stiffness, they usually have low vibration periods - below *0.5 s*. Consequently, the vibration period range from *0.2 s* to *0.5 s* is considered to be the most indicative for the evaluation of the real ductility request of the seismic sequences for this kind of structures. In the following graphs, the lines of the 95th percentiles, calculated for three different period ranges, are displayed as specified in the legend of Fig. 14.

Since the values of the ductility ratios vary consistently with the vibration period considered, a small range around the main period should be evaluated in case of more flexible structures (for instance, a range from *0.5 s* to *1.0 s* should be taken into account).

It can also be noticed how the ductility request is highly dependent on the seismic sequence. For some sequences there is no additional demand, for other sequences there is up to 74% additional demand. For this reason, the 95th percentile is calculated also for each group of sequences separately (see Table 7).

By a conservative standpoint, the values of increased ductility should be taken from the results found for all the sequences together.

Supposing that steel braced frames have a vibration period below *0.5 s*, the collected results suggest designing structures with X bracings using a behaviour factor of $q = 4$ and considering a ductility increased by

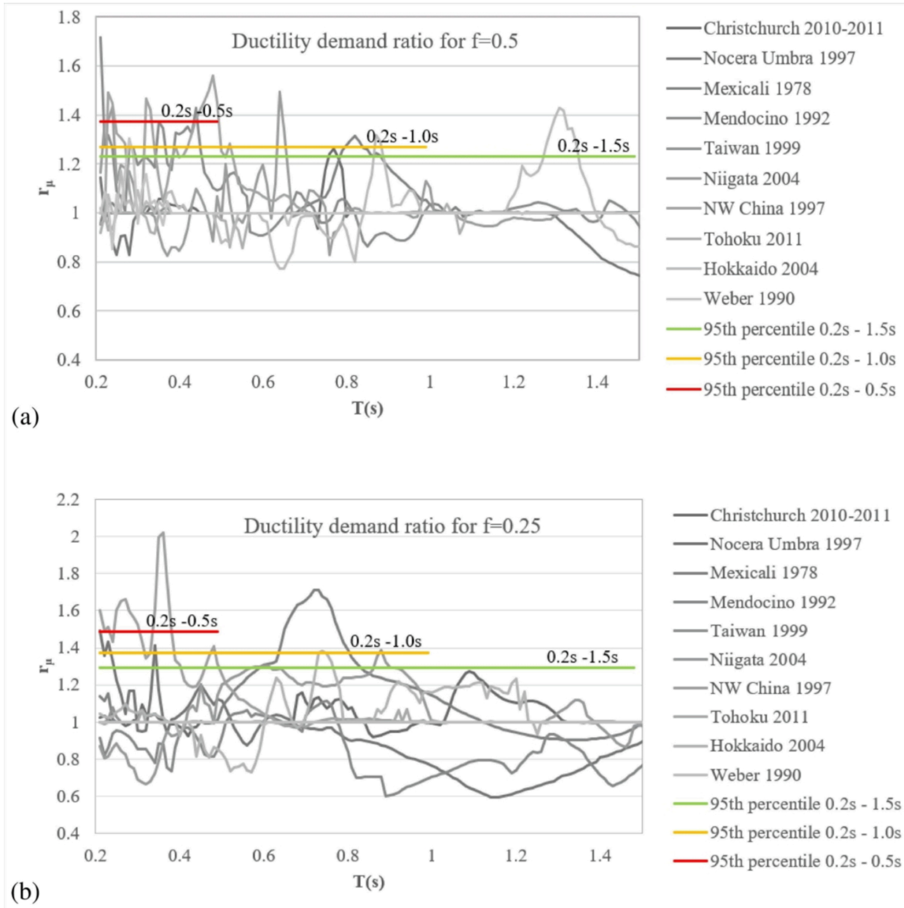

Fig. 14. Graphs of the ductility demand ratios for SDOF systems with strength reduction factors $f = 0.5$ (a) and $f = 0.25$ (b).

Table 7
Increases in ductility demand due to seismic sequences, estimated for different vibration period ranges and for different strength reduction factors, together and divided by category of sequence (group A, B and C).

Vibration period range	95th percentile of μ ratios f = 0.5	f = 0.25	Ductility increase f = 0.5	f = 0.25
	All the sequences			
0.2 s – 0.5 s	1.37	1.49	37%	49%
0.2 s – 1.0 s	1.27	1.37	27%	37%
0.2 s – 1.5 s	1.23	1.29	23%	29%
	Group A			
0.2 s – 0.5 s	1.05	1.04	5%	4%
0.2 s – 1.0 s	1.18	1.12	18%	12%
0.2 s – 1.5 s	1.06	1.20	6%	20%
	Group B			
0.2 s – 0.5 s	1.35	1.35	35%	35%
0.2 s – 1.0 s	1.30	1.54	30%	54%
0.2 s – 1.5 s	1.26	1.40	26%	40%
	Group C			
0.2 s – 0.5 s	1.42	1.56	42%	56%
0.2 s – 1.0 s	1.27	1.34	27%	34%
0.2 s – 1.5 s	1.22	1.29	22%	29%

49% compared to the one needed by the single event. If a behaviour factor $q = 2$ is chosen (when using slender or not dissipative bracings for example), then the ductility should be increased less – by 37%.

Comparing the results found in this work with the ones collected in [16], it can be seen how the seismic response of the analysed SDOF systems, with the hysteretic rule given by the OpenSees library, is pretty similar to the behaviour of the Pivot hysteretic rule with $\alpha = 10$ and $\beta = 0.20$ (PIV) used in [16].

6.1. *Additional classification of seismic sequences*

As an additional result, from the analyses of the SDOF systems with the hysteretic behaviour described in the previous section, it was found that the classification of the seismic sequences given at the beginning has an evidence also in the results of the ductility demand, as already found in [16] for the Elasto-Plastic (EPP) law. In particular, for the group:

A – the ductility demand by the seismic sequence is almost equal to the one required by one single event in the investigated range of periods. The other events have much lower ductility demand (see Fig. 15);

B – the ductility demand by the seismic sequence is almost equal to the one required by one single event just for a limited natural vibration period range (see Fig. 16);

C – the ductility demand by the seismic sequence is different from the one required by the single events, all over the vibration period range, as shown for the seismic sequence of Niigata (see Fig. 17).

7. Conclusions

In this paper, a study about the additional ductility requested by seismic sequences on single storey concentric X-braced steel frames, a very common construction system for industrial buildings, is presented. Several analyses on well-known seismic sequences have been conducted by using SDOF systems that are representative of the seismic behaviour of this kind of structures. In order to follow the hysteretic behaviour of these MDOF systems, their cyclic rule has been modelled with the “Hysteretic Uniaxial Material” available in the OpenSees framework. This hysteretic law is suitable for representing the pinching effect, typical of braced frames, and to model consistently the energy

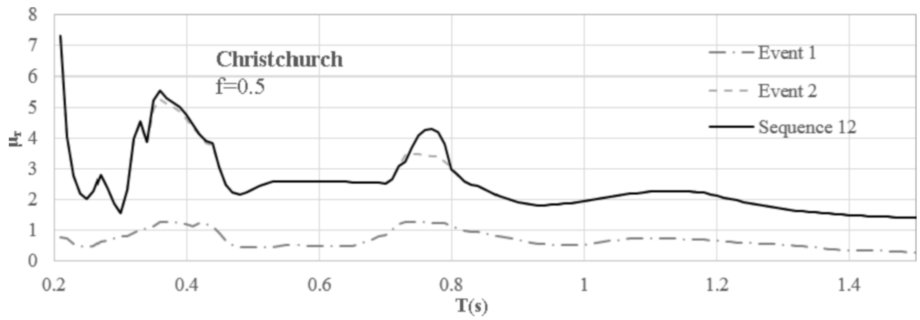

Fig. 15. Ductility demand by the seismic sequence of Christchurch and by its single events, with $f = 0.5$.

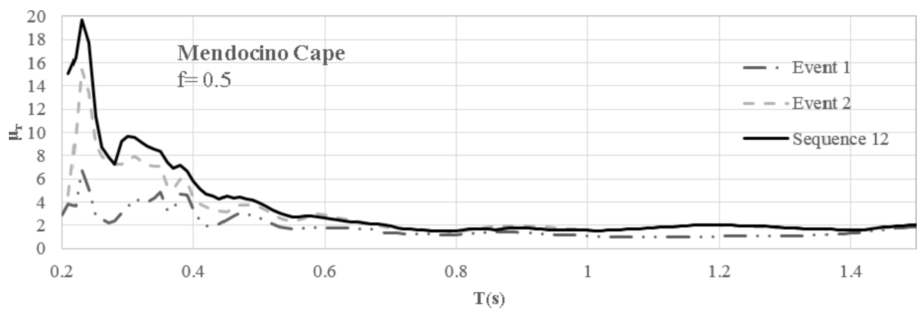

Fig. 16. Ductility demand by the seismic sequence of Nocera Umbra and by its single events, with $f = 0.5$.

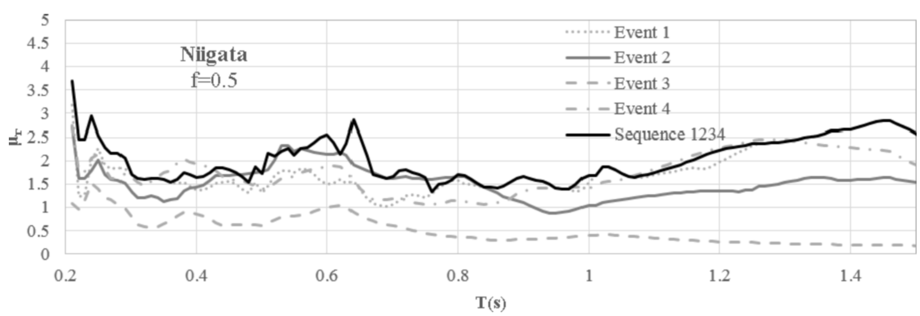

Fig. 17. Ductility demand by the seismic sequence of Niigata and by its single events, with $f = 0.5$.

dissipation. The choice of the hysteretic parameters has been verified by the comparison of the displacement demand and shape of cycles collected from SDOF and MDOF systems. After setting the parameters, the SDOF systems have been analysed with different vibration periods to obtain results on the whole response spectrum, from 0.2 s to 1.5 s. To make sure that the SDOF systems plasticise under the action of all seismic sequences, the yielding force of each system has been set as a fraction of the elastic force required by the elastic spectrum. This fraction has been purposely set to $f = 0.5$ and $f = 0.25$, equal to the inverse of behaviour factors q of 2 and 4, respectively. To calculate the additional ductility for both levels of resistance and for all the analysed vibration periods, the ratio r_μ between the ductility required by the seismic sequence and the one required by the envelope of the single seismic events has been assumed as a reference. It was found that single storey concentric X-braced steel frames should be designed with a ductility capacity that is 49% or 37% higher than the one required by the single earthquake, respectively for $f = 0.25$ and $f = 0.5$. The same result can be obtained by reducing the behaviour factor q of the same percentage and maintaining the ductility determined for one single earthquake, as already suggested in [16].

Declaration of Competing Interest

The authors declare that they have no known competing financial interests or personal relationships that could have appeared to influence the work reported in this paper.

References

[1] CEN, European Committee for Standardisation TC250/SC8/. Eurocode 8: Design Provisions for Earthquake Resistance of Structures, Part 1.1: General rules, seismic actions and rules for buildings, EN1998-1; 2003.

[2] Moustafa A, Takewaki I. (2012) *Characterization of earthquake ground motion of multiple sequences*. Earthquakes and Structures 2012;3(5):629–47.

[3] Amadio C, Fragiacomo M, Rajgelj S. The effects of repeated earthquake ground motions on the non-linear response of SDOF systems. Earthquake Eng Struct Dyn 2003;32(2003):291–308.

[4] Hatzigeorgiou GD. Ductility demand spectra for multiple near- and far-fault earthquakes. Soil Dyn Earthquake Eng 2010;30(2010):170–83.

[5] Di Sarno L. Effects of multiple earthquakes on inelastic structural response. Eng Struct 2013;56(2013):673–81.

[6] Ruiz-Garcìa J. Discussion on "Effects of multiple earthquakes on inelastic structural response". Eng Struct 2014;58(2014):110–1.

[7] Fragiacomo M, Amadio C, Macorini L. Seismic response of steel frames under repeated earthquake ground motions. Eng Struct 2012;26(2004):2021–35.

[8] Ruiz-Garcìa J, Negrete-Manriquez JC. Evaluation of drift demands in existing steel frames under as-recorded far-field and near-fault mainshock-aftershock seismic sequences. Eng Struct 2011;33(2011):621–34.

[9] Faisal A, Taksiah AM, Hatzigeoriou GD. Investigation of story ductility demands of inelastic concrete frames subjected to repeated earthquakes. Soil Dyn Earthquake Eng 2013;44(2013):42–53.
[10] Hosseinpour F, Abdelnaby AE. Effect of different aspects of multiple earthquakes on the nonlinear behaviour of RC structures. Soil Dyn Earthquake Eng 2017;92 (2017):706–25.
[11] Hosseinpour F, Abdelnaby AE. Fragility curves for RC frames under multiple earthquakes. Soil Dyn Earthquake Eng 2017;98(2017):222–34.
[12] Zhang S, Wang G, Sa W. Damage evaluation of concrete gravity dams under mainshock-aftershock seismic sequences. Soil Dyn Earthquake Eng 2013;50(2013): 16–27.
[13] Trutalli D, De Stefani L, Marchi L, Scotta R. Seismic capacity of steel frames braced with cross-concentric rectangular plates: Non-linear analyses. J Constr Steel Res 2019;161:128–36.
[14] Khandelwal K, El-Tawil S, Sadek F. Progressive collapse analysis of seismically designed steel braced frames. J Constr Steel Res 2009;65(3):699–708.
[15] Ghods S, Kheyroddin A, Nazeryan M, Mirtaheri SM, Gholhaki M. Nonlinear behavior of connections in RCS frames with bracing and steel plate shear wall. Steel and Composite Structures 2016;22(4):915–35.
[16] Rinaldin G, Amadio C, Fragiacomo M. Effects of seismic sequences on structures with hysteretic or damped dissipative behaviour. Soil Dyn Earthquake Eng 2017;97 (2017):205–15.
[17] Rinaldin G, Amadio C. Effects of seismic sequences on masonry structures. Eng Struct 2018;166:227–39. https://doi.org/10.1016/j.engstruct.2018.03.092.
[18] Reinhorn AM. *Non linear Dynamic Analysis of MDOF Structures.* Department of Civil, Structural. and Environmental Engineering at University at Buffalo; 2009.
[19] Italian Ministry of Infrastructures (2018) D.M. 17-01-2018 - Italian Building Code. Gazzetta Ufficiale Serie Generale n.42 del 20-02-2018, in Italian.
[20] NIED - National Research Institute for Earth Science and Disaster Prevention, Database of the Strong-Motion Seismograph Networks (K-NET, KiK-net), Internet site: www.kyoshin.bosai.go.jp.
[21] COSMOS. Strong Motion Data Center, Internet site: strongmotioncenter.org.
[22] Luzi L, Hailemikael S, Bindi D, Pacor F, Mele F, Sabetta F. ITACA (ITalian ACcelerometric Archive): a web portal for the dissemination of italian strong-motion data. Seismol Res Lett 2008;79(5):716–22. https://doi.org/10.1785/gssrl.79.5.716.
[23] McKenna F. OpenSees: a framework for earthquake engineering simulation. Comput Sci Eng 2011;13(4):58–66.
[24] McKenna, F., e Fenves, G. L., Scott M.H. (2000) Object oriented program, OpenSees; Open System for Earthquake Engineering Simulation. http://opensees.berkeley.edu, Pacific Earthquake Engineering Center, University of California, Berkeley.
[25] Mazzoni S, McKenna F, Scott MH, Fenves GL, Jeremic B. OpenSees Command Language Manual. University of California at Berkeley, Pacific Earthquake Engineering Research Center; 2003.
[26] Jain A.K. (1978) Hysteresis behaviour of bracing members and seismic response of braced frames with different proportions. Dissertation (PH.D.) – The University of Michigan Dissertation Abstracts International.
[27] Sivaselvan M, Reinhorn AM. Hysteretic models for deteriorating inelastic structures. J. Eng. Mech. 2000.
[28] Scott, M., Filippou, F., & Mazzoni, S. (2013). Hysteretic Material. Internet site: http://opensees.berkeley.edu/wiki/index.php/Hysteretic_Material.